

Optimized four-channel Nd:glass laser system for the investigations of spherical plasma compression

S. DENUS, A. DUBIK, B. KACZMARCZYK, J. MAKOWSKI, J. MARCZAK, J. OWSIK, Z. PATRON,
M. SZCZUREK

Kaliski Institute of Plasma Physics and Laser Microfusion, P. O. Box 49, 00-908 Warszawa, Poland.

The paper presents four-channel Nd:glass high power laser system in its optimized version, based on the theoretical analysis propagation of radiation in the real laser channel, constructed in the Kaliski Institute of Plasma Physics and Laser Microfusion (IPPLM).

1. Introduction

The laser system presented in the paper was based on a four-channel laser constructed in the Kaliski Institute of Plasma Physics and Laser Microfusion, in 1976. This system was then used in experimental investigations of the laser plasma compression [1-3]. The increasing demands with respect to temporal-spatial and energy parameters of radiation aimed at realization of laser beam concentration with higher homogeneity and power density in small areas of the targets under investigation, as well as the necessity of improving the laser system efficiency justified the reason for which the existing system had to be modified according to the actual demands with respect to the experiment and to the state of knowledge corresponding to the contemporary stage of the development of big laser installations [4-7].

The works on modernization and optimization were preceded by theoretical-calculational analysis concerning, in particular, the radiation propagation in the real laser channel, taking account of basic physical phenomena occurring during the pulse propagation [8-20].

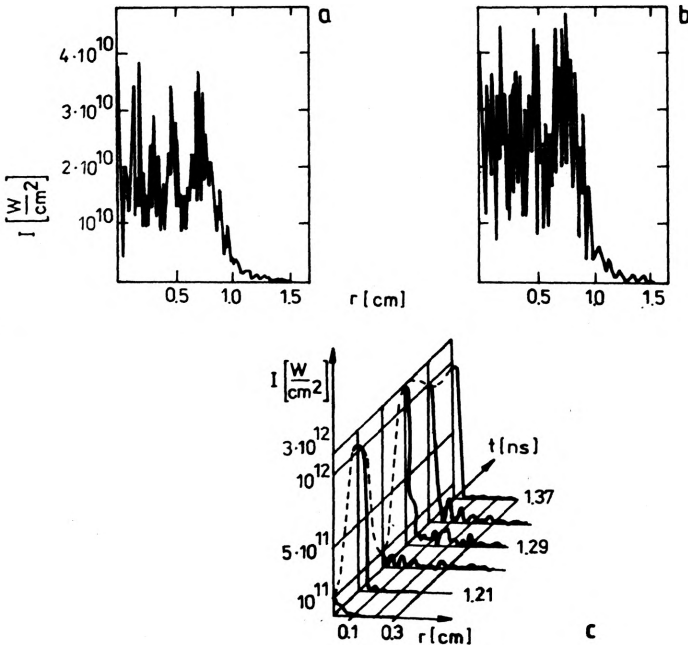
The above works were connected with the introduction of spatial vacuum filtration, apodization, relay systems and optical isolation. The efficiency of the amplifying heads was increased, as well as the reliability of the utilized electronic systems. Moreover, in order to make the laser operation more efficient, stabilization of the room temperature and the generator screening were introduced.

The laser, modernized in this way, is now operating in conditions of improved purity. The target interaction chamber was moved to a separate diagnostic room. Both the method and apparatus for spatial-temporal diagnostics and energy parameters of laser beams were improved.

2. Filtration, apodization and relaying of radiation in the high power laser system

2.1. Filtration

One of the main reasons limiting the efficiency of Nd:glass laser system is the self-focusing caused by the dependence of the index of refraction on the electric field intensity [21–27]. Usually, the whole- and small-scale self-focusing can be differentiated [4]. Small-scale self-focusing is in most cases due to inhomogeneity of the spatial structure of the beam which, in turn, is caused by radiation diffraction in the apertures of the propagation channel, by radiation interference, and by dust particles and damage spots inside or outside the optical components. This phenomenon leads to damage of the active elements, in particular internally. It also leads to a decrease of the laser efficiency as a result of the scattering of radiation on the induced phase inhomogeneities in the active medium to non-linear losses, as well as to deformation of the spatial and temporal structure of the pulse in the vicinity of the focal spot. As a consequence, laser radiation can to a considerable extent, bypass the microballoon targets used in plasma experiments, and the laser efficiency can be less than optimum. The effect of self-focusing in amplifying medium on spatial structure of a beam formed by radiation diffraction of circular aperture



[16] is illustrated in Fig. 1a, b. It can be seen, that when the mean power density in the cross-section of the beam increase, e.g., for the 11th Fresnel zone ($F = 11$), then sharp rings of high spatial frequencies and power densities exceeding many times the admissible damage threshold of optical media become more and more distinct. This leads to the time evolution of spatial structure, which has a fundamental influence on the field distribution in the vicinity of the focus spot. Changes of the field distribution in the focal spot, for this case, are presented in Fig. 1c. It can be seen that if an inhomogeneous field distribution incident on a non-linear medium is presented, then the evolution of the power density in time is expressed by the deformation of the temporal pulse shape and the displacement of the energy from zero order to higher orders. So, even this example shows the necessity of improving the efficiency and reliability of the laser system. Small-scale self-focusing can be minimized by filtration of spatial frequencies in a laser beam [27], [28]. According to [4] such a filter should remove the spatial frequencies, which are the most strongly amplified in non-linear medium described by the relation

$$K_m = \frac{2\pi}{\lambda_0} \left(\frac{2\gamma}{n_0} I \right)^{1/2}. \quad (1)$$

Thus, the following conditions must be satisfied

$$K_m > K_{co} \quad (2)$$

with

$$K_{co} = \frac{\pi D}{\lambda_0 f} \quad (3)$$

where: γ – constant characterizing the non-linear part of the index of refraction,
 n_0 – linear part of the index of refraction,
 λ_0 – wavelength in vacuum,
 K_{co} – cut-off frequency of diaphragm in focal plane of the spatial filter,
 D – diameter of diaphragm,
 f – focal length of the input lens of the filter.

Results of the experimental investigations of the spatial vacuum filter (FP-2 type) are presented in Fig. 2. They illustrate the dependence between power in the zero order of the focus and laser output power for several sizes and diameters of the filtering diaphragm [29]. The application of filter improves distinctly the beam focusing power. Thus, by applying the filtration to a high power laser system the power in zero order may be increased although the value of filter transmission T is less than one

$$T = \frac{\int_0^K KR(K) dK - \int_{K_{co}}^K KR(K) dK}{\int_0^K KR(K) dK} \times 100\% \quad (4)$$

where: K – spatial frequency including 100% of the pulse energy,
 $R(K)$ – field distribution in the spatial frequency plane of the filter.

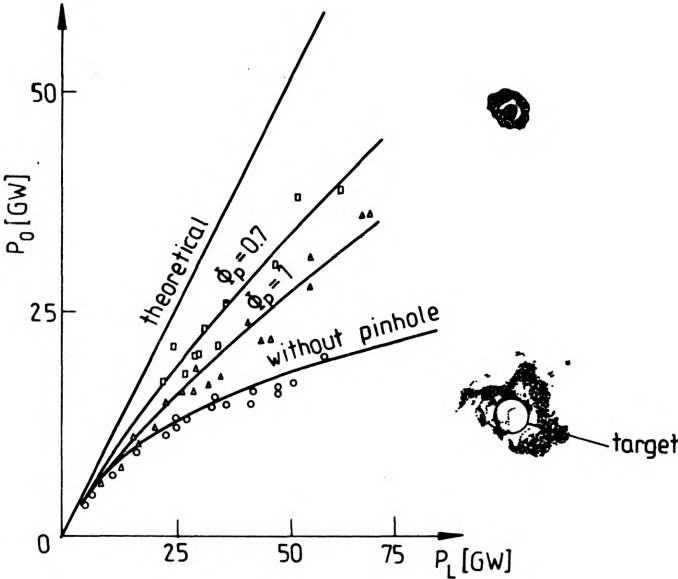


Fig. 2. Power at zero-order of focus vs output power of laser for several diameters of diaphragm Φ_p in FP 2 spatial filter [29]. P_0 – power at zero-order of focus, P_L – output laser power

The filters attenuate also both the superluminescent radiation and the lamp radiation, and at the same time increase the contrast of a laser pulse; understood as the ratio of the main pulse power to pre-pulse power.

2.2. Apodization

Spatial filtration does not prevent, however, diffraction effects generated on the apertures of diaphragm, e.g., on the apertures of the active elements in the propagation channel. Effects of such a type may be reduced by apodization, which prevents to a high degree the generation of inhomogeneities in the cross-section of the beam [30–39]. To this end soft metallic or dielectric diaphragm made by the masking method is most often used. Spatial distribution of radiation transmission through such a diaphragm is usually described by the function, called a “Super Gauss” [4]. Experimental and theoretical transmission curves of one of the dielectric diaphragms plotted for a four-channel laser are presented in Fig. 3, whereas the photographs of soft diaphragms [40] are given in Fig. 4. When a laser system contains a set of spatial filters, the choice of the appropriate value of the exponent N of “Super Gauss” function is essential. The value of the above parameters depends on such factors as whole self-focusing, efficiency of energy extraction from the amplifiers (characterized among others by the so-called aperture filling factor), diaphragming by the soft diaphragm of the field distribu-

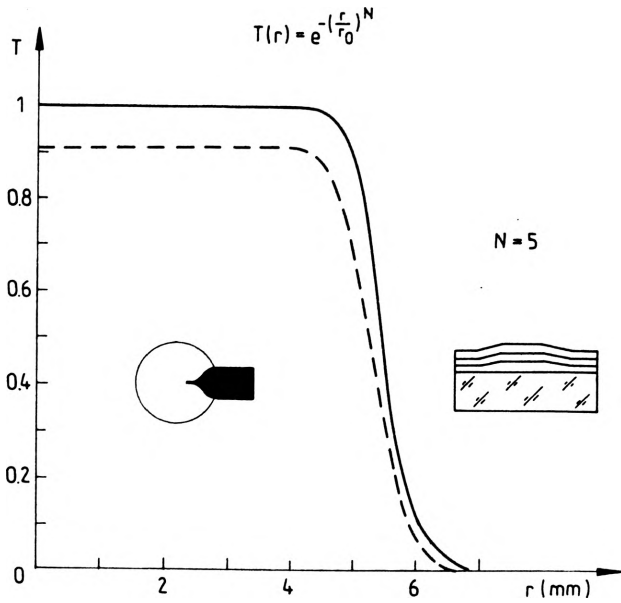


Fig. 3. Transmission characteristics of soft diaphragms [40]

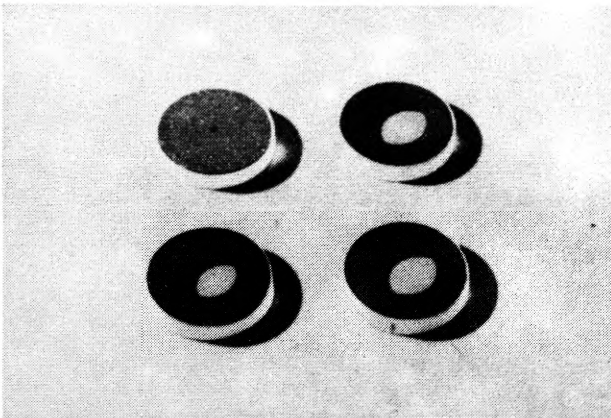


Fig. 4. Photo of soft diaphragms

tion in the separate apertures of the propagation channel and non-linearity of amplification.

Figure 5 presents the calculated evolution of a field distribution in time, in the lens focal plane, when a radial distribution of radiation characterized by the apodization parameter $N = 2$ (Fig. 5a) and $N = 128$ (Fig. 5b) was incident on a non-linear active medium [17]. It is seen that the distribution for $N = 2$ leads to much stronger spatial and temporal deformation of the pulse in the vicinity of the focal spot, than that occurring in the case of $N = 128$, when the radial field distribution is more homogeneous. If, however, distributions characterized by high values of N increases are applied, their small-scale self-focusing is more probable

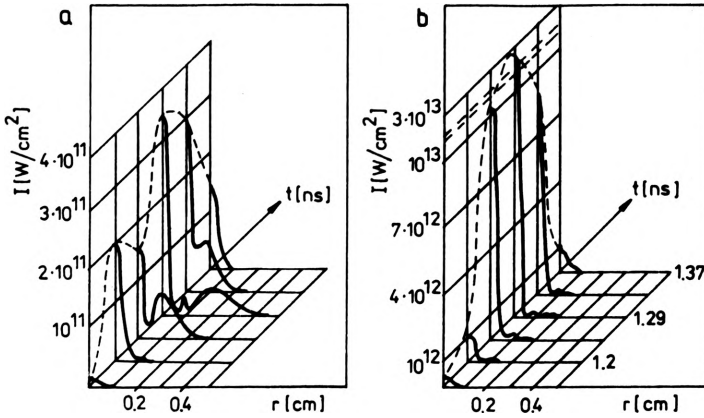


Fig. 5. Field evolution in time in the focal plane of the lens for the pulse of cross-section distribution characterized by the apodization parameters: **a** – $N = 2$, **b** – $N = 128$

because of more pronounced diffraction effects occurring in the beam. The apodization coefficient determines also the propagation distance at which the deformation of the radial distribution is significant [20].

The influence of apodization coefficient on the electric field distribution in the plane characterized by the Fresnel number $F = 5$ (for $N = 5$, and $N = 10$) is shown in Figs. 6a and 6b, respectively. It is seen that at the same distance from the initial plane $z = 0$, the distribution for $N = 10$ becomes more inhomogeneous than that for $N = 5$. At the same time the aperture filling factor increases with the apodization coefficient N [5]

$$F_f = \frac{2 \int_0^R I(r) r dr}{I_{\max} R^2} \tag{5}$$

where: $I(r)$ – spatial distribution of electric field,

R – radius corresponding to the given diaphragming height,

which thereby contributes to the increasing efficiency of energy extraction from the amplifying media [41].

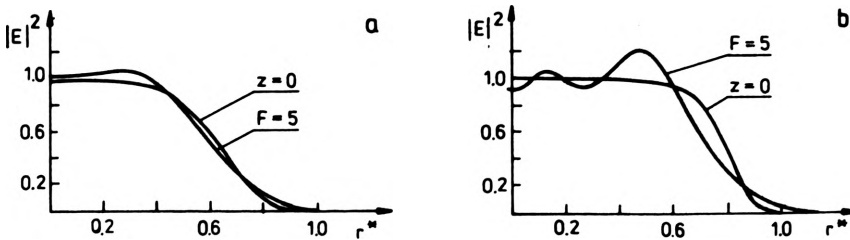


Fig. 6. Field distribution in the plane characterized by the Fresnel number $F = 5$ for the apodization coefficient: **a** – $N = 5$, **b** – $N = 10$, (r^* – normalized beam radius)

In conclusion, it can be said that the “harder” field distribution (higher N) in the laser beam is better as far as both the efficiency of energy extraction from amplifiers and minimization of the influence of whole self-focusing on the evolution of field parameters in the vicinity of focus are concerned. This statement is valid for small propagation distances (high F), within which the diffraction effects leading to the above mentioned disadvantageous effects of self-focusing on the field parameters, are minimal.

2.3. Relaying

A high power laser is of length of several tens of meters, thus its field distribution is “hard”, and practically of no use for the reasons mentioned above. These contradictions may be reconciled by taking advantage of another property of the filter, namely the relaying of the field distribution, given by means of a soft diaphragm, from the beginning of the laser system to its output plane [42-44].

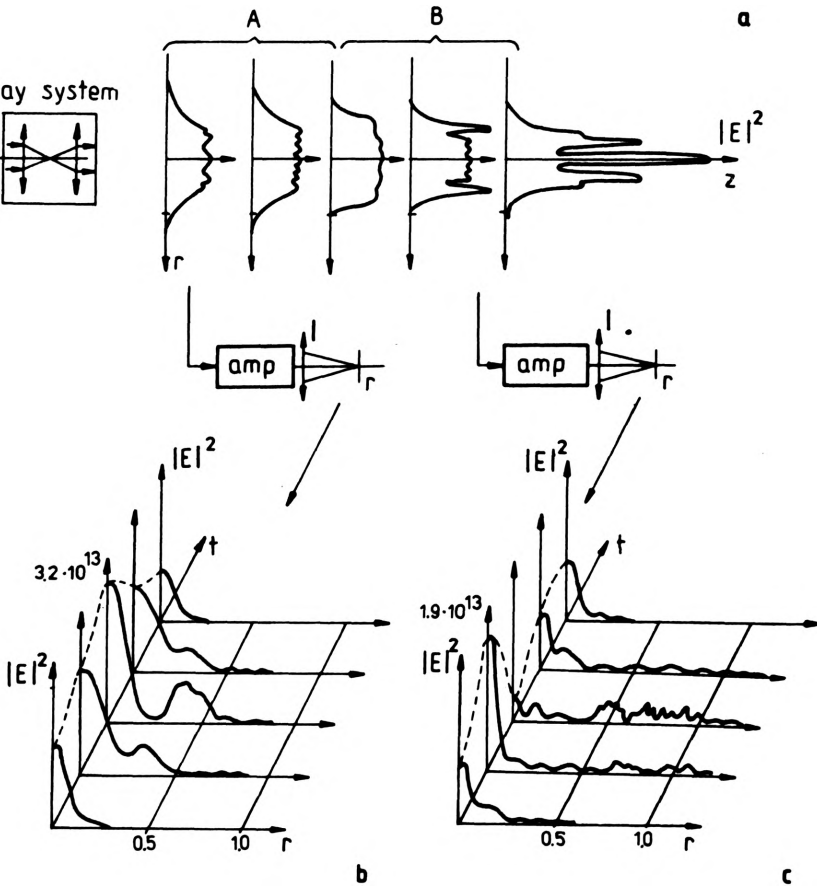


Fig. 7. Illustration of two characteristic areas of the relay system (a), and field evolution in the vicinity of the focal spot for the above areas (b, c) [18]

Relation

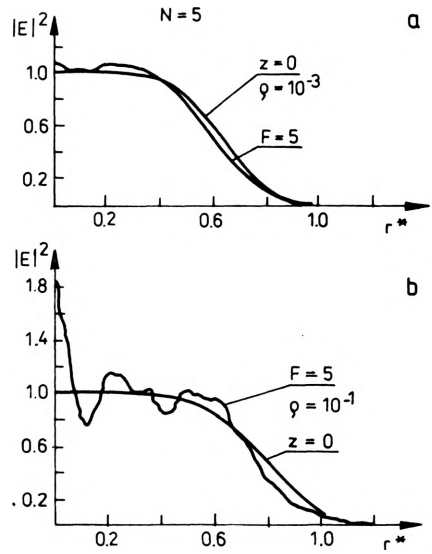
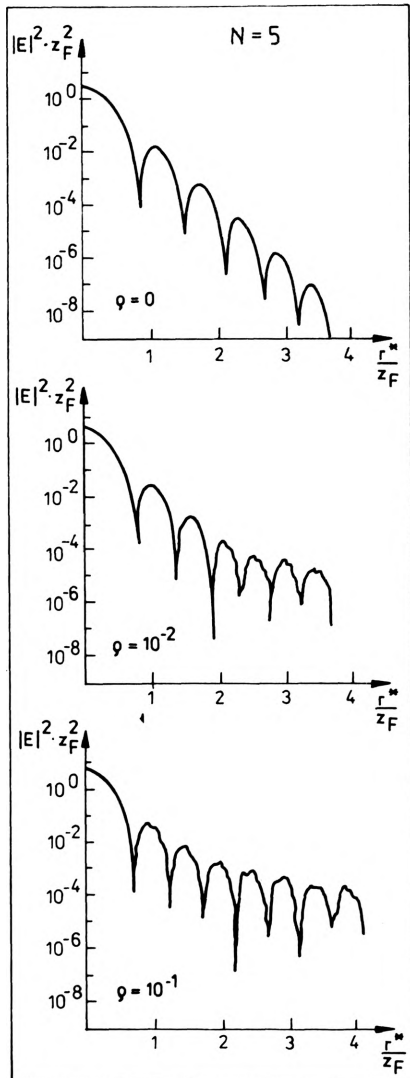
$$md_1 + \frac{d_2}{m} - f_1 - f_2 = 0 \tag{6}$$

where

$$m = f_2/f_1 \tag{7}$$

makes it possible to determine the position of the image d_2 behind the relay system, the distance of the distribution from the input plane of the relay system d_1 and its focal lengths f_1 and f_2 being given.

Two calculated characteristic areas of the relay system are presented in Fig. 7a. In the first area (marked by A) the field propagates from the input plane to that of



▲ Fig. 9. Diaphragming height vs field distribution for: $\rho = 10^{-3}$ (a) and $\rho = 10^{-1}$ (b)

◀ Fig. 8. Diaphragming height of the field distribution subject to relaying vs radiation power distribution for $N = 5$

the image with a minimal deformation of spatial structure, while in the second region (**B**) this deformation is much stronger. Thus the amplifiers cannot be placed in the channel arbitrarily, as shown in Figs. 7b and 7c, which illustrate the field evolution in the focus vicinity in these two cases [18]. Another task of the relay system is to match the aperture filling factors for the amplifying stages preceding the relay system and for the successive stages behind it, in such a way that this distribution diaphragming the aperture of active media occurred on the level not higher than 10^{-3} of the field values in the central area of the distribution.

Results of calculations of the effect of the diaphragming height of field distribution undergoing relaying in the system are illustrated in Fig. 8 for $N = 5$. It can be seen that with the increasing height of the distribution diaphragming $\varrho = |E(z = 0, r^* = 1)|^2 : |E(z = 0, r^* = 0)|^2$ the quantity of energy falling to higher orders increases and the field distribution is more strongly deformed (see Fig. 9a, b, for $N = 5$ [20], where r^* is a normalized radius of the beam, and z_F – normalized focal length of the lens).

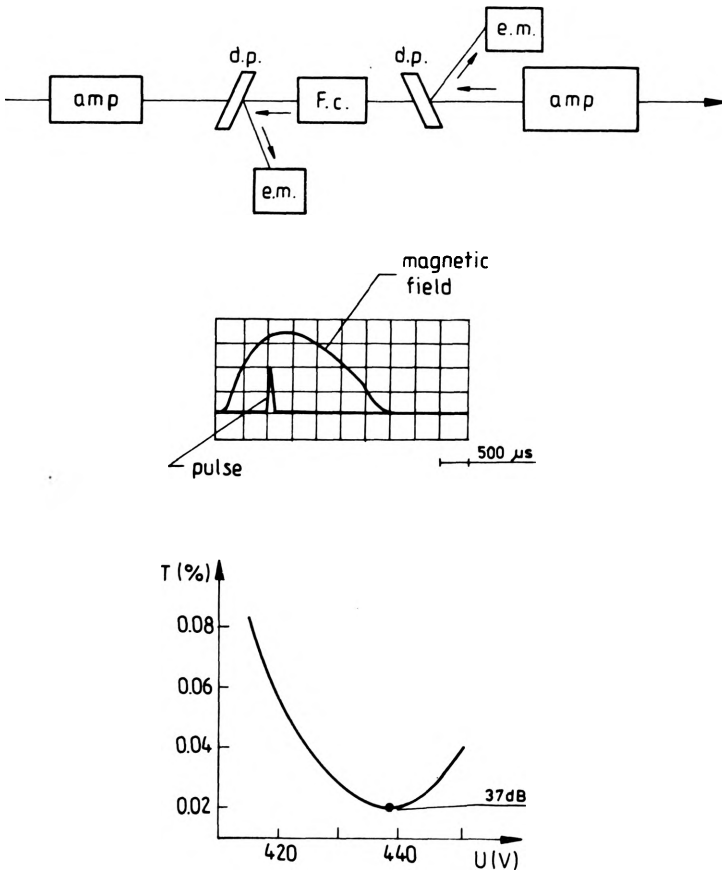


Fig. 10. Set-up and transmission characteristic of Faraday's isolator vs supply voltage from the capacitors banks for plasma reflected radiation [47]: amp – amplifier, e.m. – energy meter, d.p. – dielectric polarizer, F.c. – Faraday cell

It has been assumed in the literature [26], [27] that, in the case of self-focusing discontinuity integral B is the measure of the amplification of the most strongly increasing spatial frequencies

$$B = k_0 \gamma_0 \int_0^L I(z) dz < B_{cr} \tag{8}$$

where: $k_0 = 2\pi/\lambda$, B_{cr} – critical value characteristic for the given type of glass. In a laser system, this parameter is usually employed for determining the sites at which spatial vacuum filters are to be placed.

2.4. Optical isolation

While focusing laser radiation on targets it is necessary to protect the laser system from radiation reflected by the plasma. To this end we use Faraday’s isolator (IF) [45], [46] which at the same time prevents self-excitation of amplifiers. A scheme and transmission characteristic of the IF system of the plasma reflected radiation are shown in Fig. 10 [47].

3. Laser system

An optimized four-channel Nd glass laser system is schematically presented in Fig. 11. It consists of a generator, preamplifiers and a main amplifier with additional

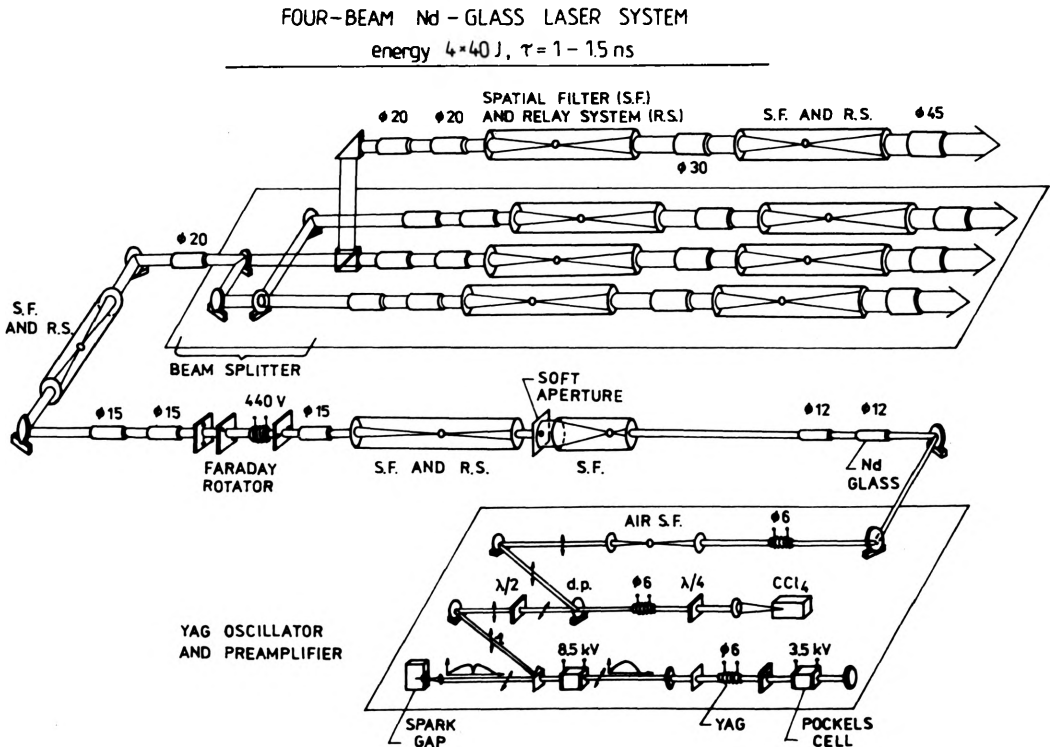


Fig. 11. Scheme of four-channel glass Nd laser system

systems improving the beam quality. The results obtained from the theoretical analysis presented above were used in design and construction of this system.

3.1. Laser generator

Scheme of the generator with a sequence of preamplifiers is presented in Fig. 12. A YAG rod of dimensions $\varnothing 6 \times 65$ mm pumped by a spiral lamp is the active material. The lamp placed in the head is surrounded with a diffusive reflector covered with a porcelain layer. Such a structure guarantees a homogeneous pumping of active medium. Resonator of the generator on YAG of the length $L_{opt} = 120$ cm consisted of two dielectric mirrors of the transmission coefficients $T = 0\%$ and 90% and the radii of curvature $R = 500$ cm and $R = \infty$, respectively. The active Q-switch is by means of the Pockels cell of P-121X type, controlled by quarter-wave voltage $U = 3.5$ kV. The system generates pulses of duration $\tau = 25$ ns (Fig. 13a) with the frequency changing from 1 to $1/3$ Hz in the basic transverse mode TEM_{q00} , output energy 30 mJ and contrast 10^{-3} . Spatial stability

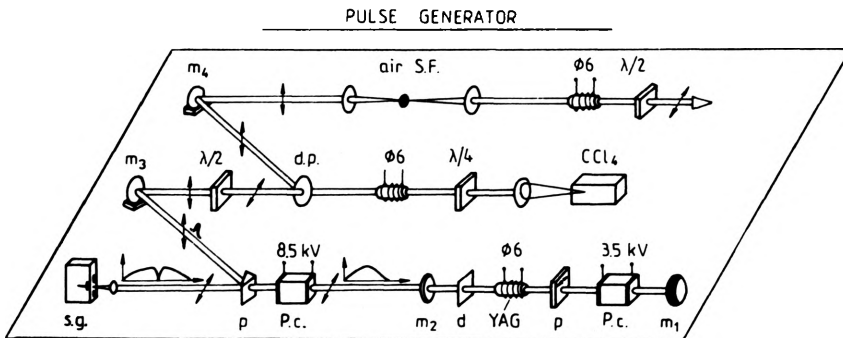


Fig. 12. Scheme of the generator and system of preamplifiers: $m_{1,3,4}$ – 100 percent reflectance mirror, m_2 – transmission mirror, P.c. – Pockel's cell, p – polarizer, d.p. – dielectric polarizer, d – diaphragm, s.g. – spark gaps, $\lambda/4$ – quarter-wave plate, $\lambda/2$ – half-wave plate, S.F. – spatial filter, CCl_4 – SBS mirror

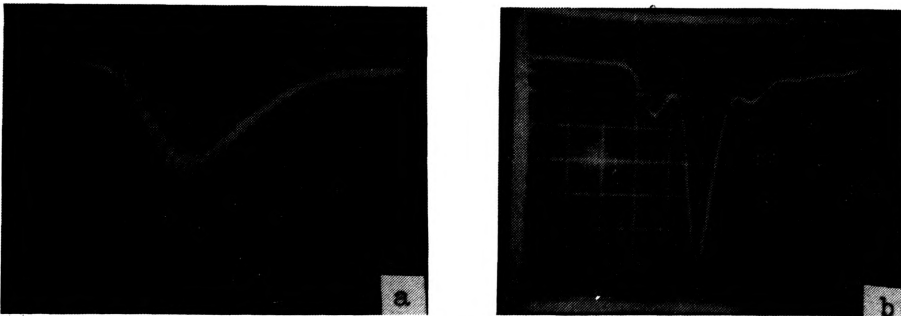


Fig. 13. Laser pulse oscillograms from: a – generator, b – after the cut-off system

of the direction of generator beam propagation amounts to 10^{-5} rad. This pulse is subjected to further temporal processing that yields the pulses ranging from 1 to 10 ns, according to the actual requirements (Fig. 13b). The pulse is cut out by the Pockels cell P-122X system, $U_{\lambda/2} = 8.8$ kV, with a spark gap initiated by a laser pulse. The cell operates in the system in which the gate of $\lambda/2$ voltage is applied for the time equal to the duration of cut-out pulse. The latter after having passed through the half-wave plate is amplified in preamplifier on the YAG.

By applying the SBS (stimulated Brillouin scattering) mirror, the pre-pulse is attenuated and the laser pulse of contrast 10^{-7} is achieved. A scheme of the system with SBS mirror and the oscillograms of the obtained laser pulses are presented in Fig. 14. The pulse of energy $E = 30$ mJ formed in this way passes through a spatial air filter and is amplified in the YAG amplifier, for which the amplification of a small signal is of the order of 20. For example, for the pulse duration 1–1.5 ns the output energy of the beam behind the sequence of pre-amplifier is equal to 150 mJ, the beam divergence is $\Theta \leq 1$ mrad and the contrast 10^{-7} .

By applying additionally a non-linear absorber it was possible to obtain in the laser system output the contrast of the order of 10^{-9} . The system of generator with the heads of amplifiers is placed on a temperature-stabilized granite plate. Both the granite plate and the whole room in which the pre-amplifiers are placed are kept at $25 \pm 0.5^\circ\text{C}$. It should be mentioned that in the above system single pulses the duration of which ranges from 20 to 150 ps may be generated by using in a generator, a cell with a non-linear absorber for passive mode locking and an output mirror of a suitable thickness. General view of the generator is presented in Fig. 15.

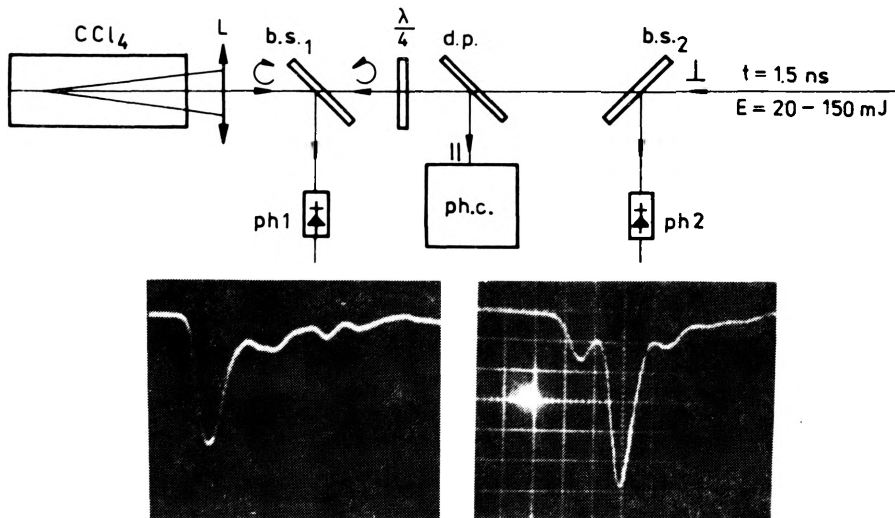


Fig. 14. System of SBS mirror: ph — photodiode, b.s. — beam splitter, d.p. — dielectric polarizer, ph.c. — camera

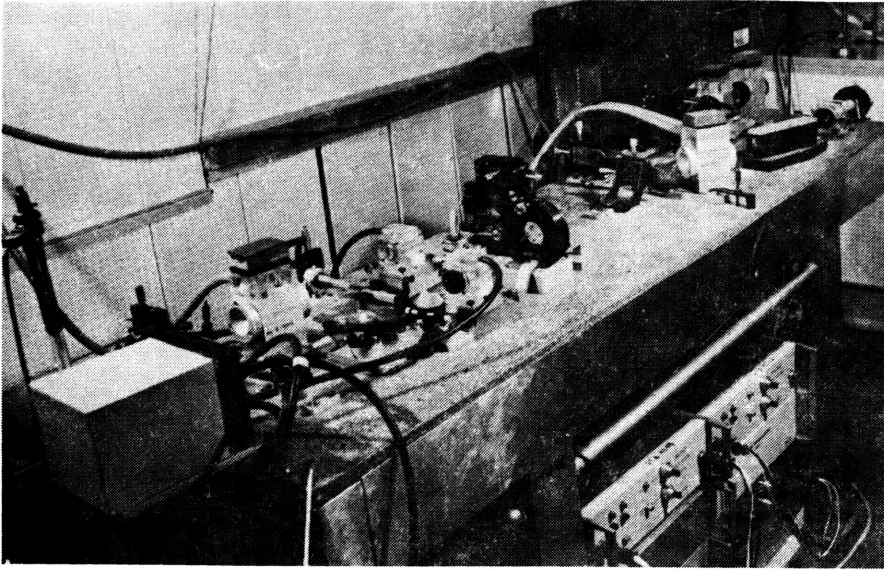


Fig. 15. General view of generator

3.2. Main amplifier

As an active material in the amplifying head the neodymium glass of the type GLS-1 is used. Immediately after the sequence of pre-amplifiers the pulse is amplified in two heads GL 220 × 12 to the level of 0.5 J. In order to eliminate the small-scale structure of the field, the beam passes through a vacuum FP-0 filter and is magnified to the diameter of 4.5 cm. The central homogeneous part of the beam, falls on the surface of soft (or hard) diaphragm of the diameter of 0.8 cm which transmits about 10% of the incident energy. This allows us to obtain the distribution of a high filling factor which is next subject to further relaying to the main surface of focusing lenses in the experimental chamber. Transmission of FP-0 filter changes depending on the incident energy (Tab. 1). A vacuum spatial filter FP-1 is placed behind the plane of soft (hard) diaphragm. Transmission of this filter ranged within 85–93%, depending on the incident energy. The FP-1 filter performs also the part of the image relay system by relaying the initial distribution through 3 heads GL 220 × 15 and the Faraday's isolator system on the input to the next vacuum spatial filter FP-2. Since each consecutive filter magnifies the

Table 1

E_{in} [J]	0.679	1.178	1.314
E_{out} [J]	0.606	0.826	0.857
T [%]	89	70	65

beam, its output diameter is 4.5 cm. Thus, the average power density in the beam in all the heads is kept below the damage threshold of active medium. The parameters of spatial filters are presented in Tab. 2.

Table 2

Type of filter	f'_1 [cm]	f'_2 [cm]	Φ_p [mm]	β	T [%]
FP-0	24.5	88.9	0.365	3.62	88
FP-1	127.7	190.9	1.5	1.49	97
FP-2	88.9	110.8	1.3	1.25	67
FP-3	83	133.5	3	1.5	85
FP-4	88.9	133.5	2.5	1.5	85

(f'_1 – focal length of the input lens, f'_2 – focal length of the output lens, Φ_p – diameter of diaphragm in filter, T – filter transmission, β – magnification)

While choosing the diameters of rods the damage threshold, given by the formula [48]

$$E_{lim} = E_0(\tau/\tau_0)^{1/2} \quad (9)$$

(where: $\tau_0 = 1$ ns, $E_0 = 3$ J/cm², τ – laser pulse duration) was taken into account. All the rods were cut at the angle of 5° with respect to the optical axis of the system. The parameters of amplifying heads of the type GL-220 are given in Tab. 3.

Table 3

Type of head	Dimension of active medium \varnothing [mm]	Maximum pumping energy [kJ]	Number of LBL 14-170 lamps	Maximum total amplification
GL 220 × 12	12 × 220	14	6	10
GL 220 × 15	15 × 220	14	6	8
GL 220 × 20	20 × 220	14	6	4.5
GL 220 × 30	30 × 220	18.5	8	3.5
GL 220 × 45	45 × 220	27	12	3

Laser pulse parameters corresponding to the separate stages of the laser system for the pulse duration of 1.5 ns are presented in Tab. 4.

The value of B integral calculated for the analysed laser system is presented in Tab. 5, assuming $n_2 = 2 \times 10^{-13}$.

The maximum output power in the last amplification stage may be estimated from the relation

$$P_{max} \cong \frac{\alpha n_0 D^2}{318 n_2} B F_t \quad (10)$$

Table 4

Generator	E_{in} [J]	E_{out} [J]	I_{in} [GW/cm ²]	I_{out} [GW/cm ²]	P_{in} [GW]	P_{out} [GW]
GL 220 × 12 (2 units)	0.15	0.15	8.84×10^{-2}	0.29	0.1	0.33
FP-0	0.5	0.45	0.29	1.88×10^{-2}	0.33	0.3
Hard aperture \varnothing 8	0.45	0.045	1.88×10^{-2}	1.88×10^{-2}	0.3	0.3
FP-1	0.45	0.043	1.88×10^{-2}	1.6×10^{-2}	0.03	0.028
GL 220 × 15 (3 units) + FR	0.043	3.3	1.6×10^{-2}	1.24	1.8×10^{-2}	2.2
FP-2	3.3	3.2	1.24	0.46	2.2	1.46
GL 220 × 20	2.2	8.4	0.46	1.78	1.46	5.6
Beam splitter	8.4	1	1.78	0.21	5.6	0.66
GL 220 × 20 (2 units)	1	6.5	0.21	1.37	0.66	4.33
FP-3	6.5	4.5	1.37	0.42	4.33	3
GL 220 × 30	4.5	16	0.42	1.51	3	10.6
FP-4	16	13.5	1.51	0.56	10.6	9
GL 220 × 45	13.5	40	0.56	1.68	9	26.7

where: α — amplification coefficient,
 n_0, n_2 — linear and non-linear refractive indices,
 D — diameter of amplifier.

Table 5

Type of head	B
GL 220 × 12 (2 units)	0.24
GL 220 × 15 (3 units)	0.59
GL 220 × 20 (1 unit)	0.69
After beam splitter	
GL 220 × 20 (2 unit)	0.86
GL 220 × 30	0.6
GL 220 × 45	0.71

In the case of spatial modulation of the beam in the system, the admissible value of B , for which self-focusing destructive for the glass GLS-1 does not occur, is ~ 2.5 . Assuming for the final amplifying stages $D = 4.5$ cm, $\alpha = 0.025$ cm⁻¹, $n_0 = 1.5$, $n_2 = 2 \times 10^{-13}$ and $F_f = 0.8$ cm we get $P_{\max} = 30$ GW.

From the estimations presented above it follows that the theory in the laser system is consistent with the experiment. The general view of the main amplifier is shown in Fig. 16.

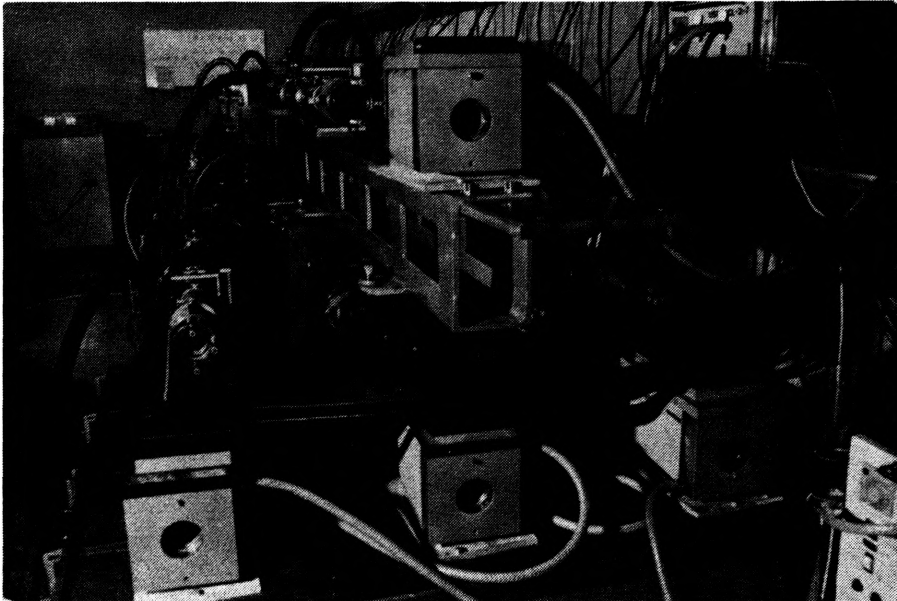
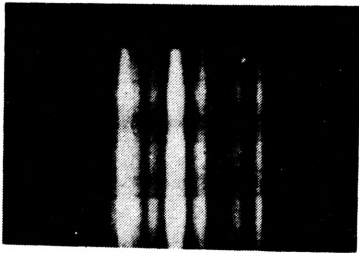
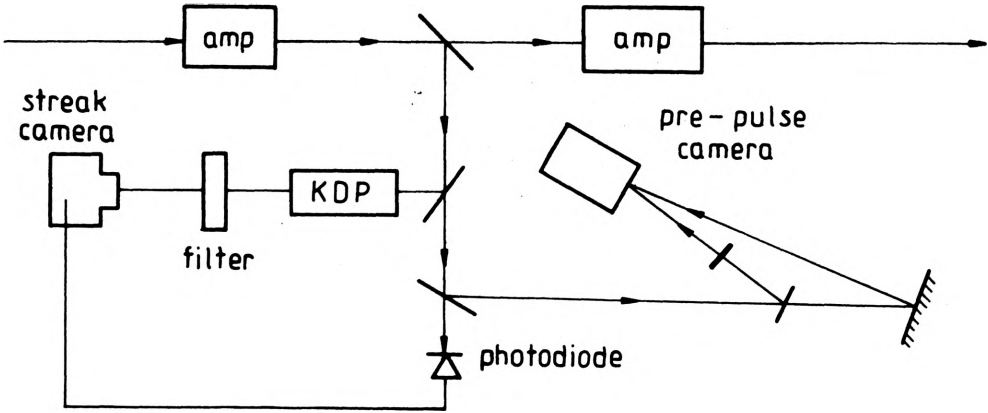


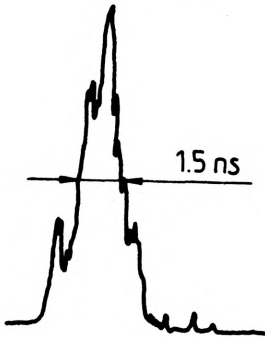
Fig. 16. General view of main amplifier

4. Beam diagnostic

The purpose of diagnostic is to obtain the information about the state of the laser system as a whole, as well as the data necessary for a complete analysis of results of plasma investigations. In the laser system discussed in the paper the diagnostic consisted in the measurements of pulse energy at different places (providing the information, concerning among others the amplification of the separate heads, total energy and the degree of danger of the medium damage), the measurements of temporal shape and pulse duration as well as of the contrast ratio.



pre-pulse record



pulse width measurements

Fig. 17. Duration and pulse contrast diagnostics

Pulse time duration was measured by a high speed camera with the pulse contrast being measured by a camera in the system presented in Fig. 17.

Figures 18a, b present near- and far-field beam diagnostics used in the laser system. The near-field diagnostic data were used for determining the sites of the local increases of power densities exceeding critical value. The far-field diagnostic provides information about the position of focus in experimental chamber as well as about the size of the focal spot, essential in power density estimation.

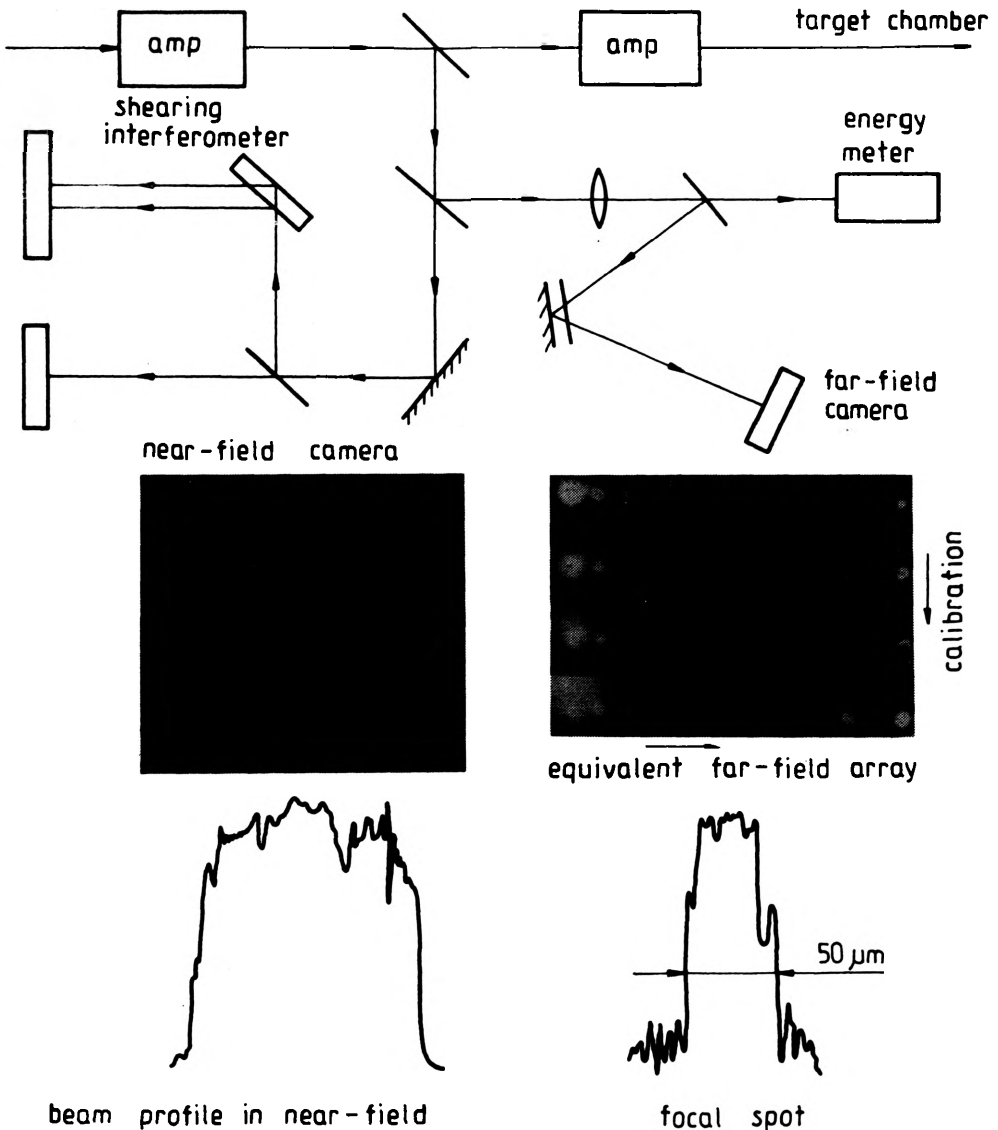


Fig. 18. Diagnostic of spatial parameters of laser beam with the use of near-field and far-field camera

In the same system the diagnostic of phase distribution in the beam cross-section is made by using a shearing interferometer, and the divergence proposed by the Hartman method.

5. Summary

An optimized four-channel Nd glass laser system presented in this paper was constructed in the Institute of Plasma Physics and Laser Microfusion. Theoretical analysis preceding the modernization and optimization allowed us to better understand the specific features of pulse propagation in the channel of high-power laser and to base the new construction of the system on the obtained information.

In the nearest future the system will be enlarged adding the heads of $\varnothing 60$, and the efficiency of the existing ones improved. Also a generator performing the acousto-optic modulation will be applied in order to increase the duration of output pulses. It is also planned to improve the system stability and pulse contrast, to construct the additional channel for X-ray backlighting, to apply the frequency conversion (to 2ω and 3ω), to introduce the optical isolators with larger apertures, and so on. The system presented in this paper is actually employed to carry out the experiments on spherical plasma compression.

References

- [1] KALISKI S., DENUS S., DUBIK A., NAGRABA S., SZYPUŁA W., WODNICKI R., WOŁOWSKI J., ZARÓWNY J., *J. Tech. Phys.* **20** (1979), 117.
- [2] KALISKI S., DENUS S., FIEDOROWICZ H., GODZIK J., NAGRABA S., RYC L., SULWIŃSKI L., SZYPUŁA W., WOŁOWSKI J., WORYNA E., *J. Tech. Phys.* **21** (1980), 3.
- [3] DENUS S., CESARZ T., FARNY J., FIEDOROWICZ H., GODZIK J., KOSTECKI J., NAGRABA S., PARYS P., PAWŁOWICZ W., RYC L., SULWIŃSKI L., WILCZYŃSKI A., WOŁOWSKI J., WORYNA E., *J. Tech. Phys.* **22** (1981), 103.
- [4] GLAZE J. A., *Opt. Engineering* **15** (1976), 118.
- [5] SEKA W., SOURS J., O. LEWIS, BEMKENBURG J., BROWN D., JACOBS S., MOUROU G., ZIMMERMAN J., *Appl. Opt.* **19** (1980), 409.
- [6] BABICHENKO S. M., BYKOVSKII N. E., SENATSKII YU. V., *Kvantovaja Elektronika* **9** (1982), 161.
- [7] FLECK J. A., JR. MORRIS J. R., BLISS E. S., *IEEE J. Quant. Electron.* **QE-14** (1978), 953.
- [8] DUBIK A., *J. Tech. Phys.* **19** (1978), 235.
- [9] DUBIK A., *ibidem*, p. 257.
- [10] DUBIK A., KIELESIŃSKI M., *J. Tech. Phys.* **19** (1978), 283.
- [11] DUBIK A., FIRAK J., *J. Tech. Phys.* **19** (1978), 383.
- [12] DUBIK A., JACH K., OWSIK J., *J. Tech. Phys.* **20** (1979), 63.
- [13] DUBIK A., JACH K., OWSIK J., *Optica Applicata* **10** (1980), 219.
- [14] DUBIK A., JACH K., *J. Tech. Phys.* **20** (1980), 161.
- [15] DUBIK A., JACH K., BADZIAK J., *J. Tech. Phys.* **20** (1980), 441.
- [16] DUBIK A., *J. Tech. Phys.* **22** (1981), 3.
- [17] DUBIK A., *ibidem* **23** (1982), 299.
- [18] DUBIK A., SZCZUREK M., *J. Tech. Phys.* **25** (1984), 257.
- [19] DUBIK A., SZCZUREK M., *ibidem*, p. 265.
- [20] DUBIK A., SARZYŃSKI A., *ibidem*, p. 279.
- [21] KELLY P. L., *Phys. Rev. Lett.* **15** (1965), 1005.
- [22] GLASS A. J., GEUNTER A. H., *Laser Induced Damage in Optical Materials*, Part I, NBS Spec. Publ. No. 387, 1973.

- [23] CAMPILLO A. J., SHAPIRO S. L., SUYDAM B. R., *Appl. Phys. Lett.* **23** (1973), 628.
- [24] FLECK J., LAYNE C., *Appl. Phys. Lett.* **22** (1973), 467.
- [25] BARANOVA N. B., BYKOVSKII, N. E., ZELDOVICH B. A., SENATSKII Yu. V., *Kvantovaya Elektronika* **1** (1974), 2433 (in Russian).
- [26] BLISS E. S., HUNT J. T., RENARD P. A., SOMMARGREN G. E., WEAVER H. J., *IEEE Quant. Electron.* **QE-12** (1976), 402.
- [27] GUIYOT J. C., BETTINGER A., AURIC D., *Rev. Phys. Appl.* **13** (1978), 198.
- [28] *Laser Program*, Annual Report, Lawrence Livermore Laboratory, 169, 1974.
- [29] CHŁODZIŃSKI J., DUBIK A., FIRAK J., MARCZAK J., OWSIK J., PATRON Z., RYCYK A., SZCZUREK M., *J. Tech. Phys.* **22** (1981), 131.
- [30] CAMPILLO A. J., PEARSON J. E., SHAPIRO S. L., TERREU N. J., *Appl. Phys. Lett.* **23** (1973), 85.
- [31] COSTICH V. R., JOHANSON B. C., *Laser Focus* **9** (1974), 3.
- [32] CAMPILLO A. J., CARPENTER B., NEWMAN B. E., SHAPIRO S. L., *Opt. Commun.* **10** (1974), 313.
- [33] HADLEY R. G., *IEEE J. Quant. Electron.* **QE-10** (1974), 603.
- [34] *Laser Program*, Annual Report, Lawrence Livermore Laboratory, 7-70, 1982.
- [35] DIELS J. C., *Appl. Opt.* **14** (1975), 2810.
- [36] KRASYUK I. K., LUKISHEVA S. T., PASHININ P. P., PROKHOROV A. M., SHIRKOV A. V., *Kvantovaya Elektronika* **3** (1976), 1337 (in Russian).
- [37] FELDMAN B. J., GITOMER S. J., *Appl. Opt.* **15** (1976), 1379.
- [38] PENZKOFER A., FRÖHLICH W., *Opt. Commun.* **14** (1978), 197.
- [39] BRODOV M. E., KAMENEC F. F., KOROBKIN V. V., PROKHOROV A. M., SEROV R. V., *Kvantovaya Elektronika* **6** (1979), 377 (in Russian).
- [40] DUBIK A., FIRAK J., JACH K., Report of the Institute of Plasma Physics and Laser Microfusion, No. 4/80/24.
- [41] *Laser Program*, Annual Report, Lawrence Livermore Laboratory, 1976.
- [42] HUNT J. T., RENARD P. A., SIMMONS W. W., *Appl. Opt.* **16** (1977), 779.
- [43] HUNT J. T., GLAZE J. A., SIMMONS W. W., RENARD P. A., *Appl. Opt.* **17** (1978), 2053.
- [44] VLASOV S. N., YASHIN V. E., *Kvantovaya Elektronika* **8** (1981), 510 (in Russian).
- [45] FONG P. K., *Rev. Sc. Instr.* **F41** (1979), 1434.
- [46] BRANNON P. J., FRANKLIN F. R., HAUSER G. C., LAVASEK J. W., JONES E. D., *Appl. Opt.* **13** (1974), 1555.
- [47] FARYŃSKI A., KARPÍŃSKI L., NOWAK A., OWSIK J., Report of the Institute of Plasma Physics and Laser Microfusion, No. 16/80/19/36.
- [48] BASOV N. T., BYKOVSKII N. E., DANILOV A. E., KALASHNIKOV M. P., KROKHIN O. N., KRUGLOV B. V., MIKHAILOV Yu. A., OSETROV V. P., PLETNEV N. V., RODE A. V., SENATSKII Yu. V., SKLIZKOV T. V., FEDOTOV S. I., FEDOTOV A. N., *Trudy FIAN* **103** (1978), 8 (in Russian).

Received May 27, 1985

in revised form September 17, 1985

Оптимализированная четырёхканальная лазерная установка на неодимовом стекле, предназначенная для исследования сферической компрессии плазмы

Б работе представлена четырёхканальная лазерная установка большой мощности на неодимовом стекле, построенная в Институте Физики Плазмы и Лазерного Микросинтеза, оптимизированная на основе теоретических расчётов лазерного тракта.